80-006 IL45

Water Research Vol. 14, pp. 117 to 127
© Pergamon Press Ltd 1980. Printed in Great Britain

0043-1354/80/0201-0117$02.00/0

MASS AND HEAT TRANSFER IN A CIRCULAR TUBE WITH BIOFOULING

JOHN P. KIRKPATRICK, LARRY V. MCINTIRE
Department of Chemical Engineering, Rice University, Houston, Texas, U.S.A.

and

WILLIAM G. CHARACKLIS
Department of Environmental Science and Engineering, Rice University, Houston, TX, U.S.A.

(*Received* 16 *June* 1979)

Abstract—A mathematical model of heat and mass transfer for a fluid flowing in a hollow cylinder with a tubular biofilm is developed. Results in dimensionless form are presented for mass transfer in isothermal laminar and turbulent flow and for heat transfer and combined heat–mass transfer in turbulent flow. For each system, the dominant resistance to the transport of heat and mass is determined. In a typical heat exchanger, the presence of a biofilm is found to decrease heat transfer significantly. For systems of interest, the biofilm thickness is nearly constant over the length of the tube in isothermal turbulent flow. In tubes with combined heat and mass transfer the thickness varies appreciably with the temperature of the fluid.

INTRODUCTION

Fouling, the undesirable deposition of materials on surfaces, is a major cause of energy losses in fluid transport and heat exchange systems. The general term fouling can reflect any or all combinations of the following processes:

1. Precipitation or crystallization (scaling)—primarily due to precipitation of calcium salts on heated surfaces.
2. Sedimentation and adsorption of solid suspended particles on surfaces.
3. Corrosion—production of thermally insulating metal oxide films from corrosion processes.
4. Biological (or organic) fouling—development of a microbial film possibly followed by a succession of higher life forms.

This paper concerns the development and effects of microbial fouling films.

Microbial fouling is a major cause of energy losses in water supply pipelines. Thin biofilms, exhibiting viscoelastic properties, develop on the conduit walls causing unexpectedly large increases in fluid frictional resistance. Characklis (1973 a,b) and Norrman *et al.* (1977) have reviewed the literature concerning biofilm development and its effect on frictional resistance.

Insulating microbial films also develop in heat exchange tubes, causing reduced efficiency. Steam driven power plants, consumers of 80% of all industrial cooling water in the United States, encounter significant problems in this area. Reduced efficiency, caused by fouling in surface condensers, costs the power industry approximately $400 million per year (Ritter & Suitor, 1976). The fouling is primarily due to microbial growths and their production of extracellular polymers which accelerate adsorption of fine suspended particles on the heated surfaces.

Similar biofilm development accelerates corrosion processes on metal surfaces and influences deterioration of wood. Microbial fouling is one of the major barriers to economic utilization of ocean thermal energy conversion and membrane desalination processes.

Calculating the heat and/or mass transfer to a fluid flowing in a cylindrical tube is a classical problem in engineering. One of the earliest models employed for heat transfer in a tube is that of fully developed laminar flow of a Newtonian fluid with constant wall temperature and fluid physical properties. In 1883, Graetz (1883) first obtained a solution to this problem for bulk temperature as a function of axial distance. With the advent of modern computers, the accuracy of this solution has been improved (Brown, 1960).

Reneau *et al.* (1969, 1971) and Bruley & Knisely (1970) have numerically modeled oxygen transport in the human capillary system under conditions of steady and unsteady state with plug flow. For the highly nonlinear kinetics of oxyhemoglobin dissociation in oxygen transport, Colton & Drake (1971) have shown that the solution for the concentration profile depends strongly on the boundary conditions employed. In modeling hollow fiber enzyme reactors, Waterland *et al.* (1974) calculated Thiele moduli and concentration profiles for laminar flow in the tube and zero-order, first-order, and Michaelis–Menten kinetics in the fiber. To determine solute removal rates in an artificial membrane dialyzer, Grimsrud & Babb (1966) have obtained an analytical solution for the bulk concentration of a solute dissolved in a New-

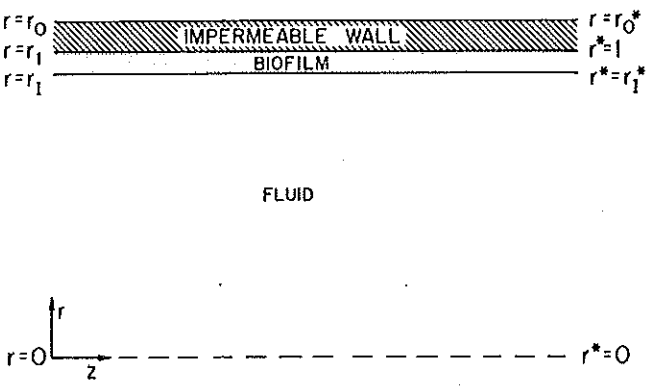

Fig. 1. Schematic diagram of circular tube with attached biofilm.

tonian fluid with laminar flow between parallel plates and a flux boundary condition at the wall.

This paper presents a phenomenological model for development of biofilm in a circular tube and its effect on heat transfer. Both laminar and turbulent flow of the fluid are examined, and variations of fluid physical properties with temperature are included.

Mass transfer

Consider the case of a Newtonian fluid moving through a hollow cylinder, the inner surface of which is coated with a biofilm that is metabolizing a dilute substrate (Fig. 1). If it is assumed that the system is axially symetric, the time-smoothed equation of mass continuity in cylindrical coordinates with constant density is written (Lightfoot, 1974)

$$\frac{1}{r}\frac{\partial}{\partial r}\left(Dr\frac{\partial c}{\partial r}\right)+\frac{\partial}{\partial z}\left(D\frac{\partial c}{\partial z}\right)+R = v_z\frac{\partial c}{\partial z}+v_r\frac{\partial c}{\partial r}+\frac{\partial c}{\partial t} \quad (1)$$

where c is the substrate concentration, D is the effective substrate diffusivity, R is the reaction rate, and v_z and v_r are the axial and radial time-smoothed velocities, respectively.

At this point, it is convenient to make several simplifications of equation (1). If the flow is assumed to be fully developed upon entering the slime-coated tube section, the biofilm thickness is very small compared to the inner radius of the tube, and the net bulk flow of fluid into the biofilm is negligible, the term containing the time-smoothed radial velocity may be discarded. Since the radial concentration gradients will be much greater than the axial concentration gradients in this system, axial diffusion is assumed to be negligible; mass transport is solely by radial diffusion and axial convection. It is reasonable to expect that the concentration profile is established much faster than the biofilm thickness changes. In this case, the time derivative in equation (1) may be dropped, and a pseudo-steady state approximation employed. These assumptions yield the simplified form of equation (1):

$$\frac{1}{r}\frac{\partial}{\partial r}\left[Dr\frac{\partial c}{\partial r}\right]+R = v_z\frac{\partial c}{\partial z} \quad (2)$$

Defining the following dimensionless variables

$$c^* = c/c_0 \quad r^* = r/r_1 \quad z^* = \frac{zD_m}{r_1^2\langle v\rangle} \quad (3)$$

where r_1 is the inner radius of the tube, $\langle v\rangle$ is the average fluid velocity in the clean tube, c_0 is the inlet concentration, and D_m is the molecular substrate diffusivity in the biofilm, in dimensionless form equation (2) is written:

$$\frac{1}{Dr^*}\frac{\partial}{\partial r^*}\left(Dr^*\frac{\partial c^*}{\partial r^*}\right)+\frac{Rr_1^2}{c_0D} = \frac{v_z}{\langle v\rangle}\frac{D_m}{D}\frac{\partial c^*}{\partial z^*} \quad (4)$$

If the reaction only occurs in the biofilm, then R will be zero in the fluid. Hence, for the fluid phase, equation (4) is written:

$$\frac{1}{D_f r^*}\frac{\partial}{\partial r^*}\left(D_f r^*\frac{\partial c^*}{\partial r^*}\right) = \frac{v_z}{\langle v\rangle}\frac{D_m}{D_f}\frac{\partial c^*}{\partial z^*} \quad (5)$$

where D_f is the sum of the turbulent and molecular diffusivities. In the biofilm, mass transfer is solely by radial molecular diffusion, and with the assumption of homogeneity, this implies that the diffusivity is constant. Thus, for the biofilm, equation (4) becomes:

$$\frac{1}{r^*}\frac{\partial}{\partial r^*}\left(r^*\frac{\partial c^*}{\partial r^*}\right) = \frac{-Rr_1^2}{c_0D_s} \quad (6)$$

where D_s is the diffusivity of the substrate in the slime. If saturation kinetics are chosen, an expression for R may be written:

$$R = -\frac{k_1c}{1+k_2c} \quad (7)$$

Putting this expression in dimensionless form yields:

$$\frac{Rr_1^2}{D_sc_0} = -\frac{k_1^*c^*}{1+k_2^*c^*} \quad (8)$$

where:

$$k_1^* = \frac{k_1 r_1^2}{D_s}$$
$$k_2^* = k_2 c_0. \tag{9}$$

The fluid is assumed to enter the tube with concentration c_0 which determines the initial condition:

$$c = c_0 \qquad z = 0. \tag{10}$$

The assumption of axial symmetry indicates a "no-flux" boundary condition at the centerline:

$$\frac{\partial c}{\partial r} = 0 \qquad r = 0 \tag{11}$$

Given the pseudo-steady state approximation, the fluxes into and out of the biofilm–fluid interface, $r = r_1$, must be equal, yielding:

$$\left(D_f \frac{\partial c}{\partial r}\right)_{-r_1} = \left(D_s \frac{\partial c}{\partial r}\right)_{+r_1} \qquad r = r_1 \tag{12}$$

The concentrations on each side of the interface must also be in equilibrium. This is described by the relation.

$$c_{-r_1} = \alpha c_{+r_1} \qquad r = r_1 \tag{13}$$

where α is the membrane partition coefficient.

If the wall of the pipe is impermeable, a "no-flux" boundary condition is again obtained:

$$\frac{\partial c}{\partial r} = 0 \qquad r = r_1 \tag{14}$$

In dimensionless form, the initial and boundary conditions are written:

$$c^* = 1 \qquad z^* = 0 \tag{15}$$

$$\frac{\partial c^*}{\partial r^*} = 0 \qquad r^* = 0 \tag{16}$$

$$\left(\frac{\partial c^*}{\partial r^*}\right)_{-r_1^*} = \left(\frac{D_s}{D_f}\frac{\partial c^*}{\partial r^*}\right)_{+r_1^*} \qquad r^* = r_1^* \tag{17}$$

$$c^*_{-r_1^*} = \alpha c^*_{+r_1^*} \qquad r^* = r_1^* \tag{18}$$

$$\frac{\partial c^*}{\partial r^*} = 0 \qquad r^* = 1 \tag{19}$$

For flow in pipes, the flow regime is characterized by a dimensionless group, Re, the Reynolds number, which is defined:

$$Re = \frac{2\langle v\rangle r_1}{\nu r_1^*} \tag{20}$$

where ν is the kinematic viscosity. When $Re < 2100$ the flow is streamline or laminar, and for laminar flow of a Newtonian fluid the velocity profile is parabolic. In this system, the velocity field is given by the expression:

$$v_z = \frac{2\langle v\rangle}{r_1^{*2}}\left[1 - \left(\frac{r^*}{r_1^*}\right)^2\right] \tag{21}$$

In this flow regime, radial mass transfer is solely by molecular diffusion, and thus, $D_f = D_m$. Hence, equation (5) is written:

$$\frac{1}{r^*}\frac{\partial}{\partial r^*}\left(r^*\frac{\partial c^*}{\partial r^*}\right) = \frac{2}{r_1^{*2}}\left[1 - \left(\frac{r^*}{r_1^*}\right)^2\right]\frac{\partial c^*}{\partial z^*} \tag{22}$$

When $Re > 2100$ the flow is turbulent and may be divided into two regions—a viscous sublayer near the interface and a turbulent core (Levich, 1962). The time-smoothed velocities, in the viscous sublayer are found from:

$$v_z = \frac{\langle v\rangle Re \cdot f(r_1^* - r^*)}{r_1^{*2} r_1^*}, \quad \frac{r_1^* - r^*}{r_1^*} < 11.6\left(\frac{2}{Re}\sqrt{\frac{2}{f}}\right) \tag{23}$$

where f is a friction factor dependent on Re and the "wall" (biofilm–fluid interface) smoothness. In the turbulent core, the velocity is determined by:

$$v_z = \frac{\langle v\rangle}{r_1^{*2}}\sqrt{\frac{f}{2}}\left[5.5 + 2.5\ln\left(\frac{Re}{2}\sqrt{\frac{f}{2}}\frac{(r_1^* - r^*)}{r_1^*}\right)\right], \quad \frac{r_1^* - r^*}{r_1^*} > 11.6\left(\frac{2}{Re}\sqrt{\frac{2}{f}}\right) \tag{24}$$

When the flow is turbulent, radial mass transfer is by both molecular and convective diffusion. Hence, the effective substrate diffusivity in the fluid is written:

$$D_f = E_D + D_m \tag{25}$$

where E_D is the turbulent diffusivity. In the turbulent core, E_D is set equal to an experimentally observed value (Sherwood *et al.*, 1975) which depends on velocity and r_1 but is independent of radial position and molecular species. For the viscous sublayer, E_D may be found from the empirical correlation (Notter & Sleicher, 1971):

$$E_D = \frac{0.0009\nu\left(\frac{Re}{2}\sqrt{\frac{f}{2}}\frac{r_1^* - r^*}{r_1^*}\right)^3}{\left[1 + 0.0067\left(\frac{Re}{2}\sqrt{\frac{f}{2}}\frac{r_1^* - r^*}{r_1^*}\right)^2\right]^{1/2}} \tag{26}$$

The equation of mass continuity in time-smoothed dimensionless variables for the turbulent core is written:

$$\frac{1}{r^*}\frac{\partial}{\partial r^*}\left(r^*\frac{\partial c^*}{\partial r^*}\right) = \frac{v_z}{\langle v\rangle}\frac{D_m}{E_D + D_m}\frac{\partial c^*}{\partial z^*} \tag{27}$$

and for the viscous sublayer:

$$\frac{1}{E_D + D_m}\frac{\partial E_D}{\partial r^*}\frac{\partial c^*}{\partial r^*} + \frac{1}{r^*}\frac{\partial}{\partial r^*}\left(r^*\frac{\partial c^*}{\partial r^*}\right) = \frac{v_z}{\langle v\rangle}\frac{D_m}{E_D + D_m}\frac{\partial c^*}{\partial z^*} \tag{28}$$

Slime growth

For modeling of slime growth, a simple mass balance is performed; i.e. it is assumed a constant proportion of the substrate entering the biofilm is converted to biomass. At a particular axial position, the mass balance for the time between t and $t + \Delta t$ is written:

$$2\beta\int_{t}^{t+\Delta t}\left(rD_f\frac{\partial c}{\partial r}\right)_{-r_f}\mathrm{d}t = \rho(r_f^{2(t+\Delta t)} - r_f^{2(t)}) \quad (29)$$

where β is the fractional yield, and ρ is the slime density. Note that at $r = r_f$, $D_f = D_m$. If the pseudo-steady state approximation is valid and a sufficiently small Δt is chosen, the flux term may be removed from the integral in equation (29) and the resulting expression integrated to yield

$$2\beta\left(\frac{r_f^{(t)} + r_f^{(t+\Delta t)}}{2}\right)\left(D_m\frac{\partial c}{\partial r}\right)_{-r_f}\Delta t = \rho(r_f^{2(t+\Delta t)} - r_f^{2(t)}) \quad (30)$$

Putting equation (30) in dimensionless form and simplifying:

$$r_f^{*(t+\Delta t)} = r_f^{*(t)} + \left(\frac{\partial c^*}{\partial r^*}\right)_{-r_f^*}\Delta t^* \quad (31)$$

where:

$$\Delta t^* = \frac{\Delta t D_m \beta C_0}{\rho r_1^2} \quad (32)$$

From Δt^* a dimensionless time, τ, may be defined

$$\tau = \Sigma\Delta t^* = \frac{t D_m \beta C_0}{\rho r_1^2} \quad (33)$$

Heat transfer

With two important exceptions, the equations of change for heat transfer and the governing boundary conditions are analogous to the mass transfer equations. The first exception is that heat produced in the biofilm is assumed negligible, and thus, R will be zero everywhere. The second is that a fluid is held at a constant bulk temperature outside of the tube. Thus, the boundary condition at the inner surface of the tube wall is:

$$-k_s\frac{\partial T}{\partial r} = U(T_0 - T_{r_1}) \quad r = r_1 \quad (34)$$

where k_s is the thermal conductivity of the slime, T_0 is the bulk temperature of the fluid on the shell side, and U is an overall heat transfer coefficient calculated from:

$$\frac{1}{Ur_1} = \left(\frac{1}{r_0 h_0} + \frac{\ln r_0/r_1}{k_w}\right) \quad (35)$$

where r_0 is the outer radius of the tube, h_0 is the heat transfer coefficient of the fluid on the shell side, and k_w is the thermal conductivity of the tube wall.

For steam condensing on horizontal tubes, h_0 is determined from the expression (Bird *et al.*, 1960)

$$h_0 = 0.725\left(\frac{-k_0^3\rho_0^3 g\Delta H_{vap}}{2\mu_0 r_0(T_{r_1} - T_0)}\right)^{1/4} \quad (36)$$

where k_0, ρ_0, and μ_0 are the thermal conductivity, density, and viscosity of the liquid film, g is the gravitational constant, and ΔH_{vap} is the heat of vaporization of the steam.

For heat transfer, dimensionless variables are defined:

$$z^* = \frac{zD_m^{(T)}}{\langle v\rangle r_1^2} \qquad r^* = r/r_1$$
$$T^* = \frac{T - T_i}{T_0 - T_i} \quad (37)$$

where T_i is the inlet temperature of the fluid and $D_m^{(T)}$ is the molecular thermal diffusivity of the fluid. Since thermal diffusivity, conductivity and density change less than 10% over the temperature ranges in typical heat exchangers, these physical properties are taken as constants.

Having defined the variables, the governing equations and conditions are written in time-smoothed dimensionless form:

$$\frac{1}{D_f^{(T)}}\frac{1}{r^*}\frac{\partial}{\partial r^*}\left[D_f^{(T)} r^*\frac{\partial T^*}{\partial r^*}\right] = \frac{v_z}{\langle v\rangle}\frac{D_m^{(T)}}{D_f^{(T)}}\frac{\partial T^*}{\partial z^*} \quad 0 \le r^* < r_f^* \quad (38)$$

$$\frac{1}{r^*}\frac{\partial}{\partial r^*}\left[r^*\frac{\partial T^*}{\partial r^*}\right] = 0 \qquad r_f^* < r^* < 1$$

$$T^* = 0 \qquad z^* = 0 \quad (39)$$

$$\frac{\partial T^*}{\partial r^*} = 0 \qquad r^* = 0 \quad (40)$$

$$T^*_{-r_f^*} = T^*_{+r_f^*} \qquad r^* = r_f^* \quad (41)$$

$$\left(\frac{\partial T^*}{\partial r^*}\right)_{-r_f^*} = \frac{k_s}{k_f}\left(\frac{\partial T^*}{\partial r^*}\right)_{+r_f^*} \qquad r^* = r_f^* \quad (42)$$

$$\frac{\partial T^*}{\partial r^*} = \frac{Ur_1}{k_s}(1 - T^*_{r^*=1}) \qquad r^* = 1 \quad (43)$$

where k_f is the thermal conductivity of the fluid.

It is useful to recognize that the boundary condition at $r^* = 1$ yields the local Nusselt number, Nu_{loc}, defined by:

$$Nu_{loc} = \left(\frac{\partial T^*}{\partial r^*}\right)_{r^*=1} = \frac{Ur_1}{k_s}(1 - T^*_{r^*=1}) \quad (44)$$

A space averaged Nusselt number, Nu_{sa}, may also

be found, using:

$$Nu_{t_a} = \frac{\int_0^{z^*} Nu_{loc}\, \partial z^*}{z^*} \tag{45}$$

Coupled heat and mass transfer

As stated in the previous section, density, thermal diffusivity, and thermal conductivity change negligibly over the temperature ranges encountered in this study. However, the mass diffusivity, viscosity, and reaction rate are strongly temperature dependent. To calculate the mass diffusivity, the simple rule is employed (Perry, 1963).

$$\frac{D\mu}{T} = \text{constant} \tag{46}$$

Thus, knowing the diffusivity at one temperature and viscosity as a function of temperature, the diffusivity at "any" temperature can be determined.

The temperature dependent reaction rate is taken to be of the form:

$$\frac{R(T)}{R(T_e)} = A \exp\left(\frac{-E}{T}\right) - A' \exp\left(\frac{-E'}{T^2}\right) \quad T < T_D$$
$$= 0 \quad T > T_D \tag{47}$$

where T_e is the temperature at which the reaction rate is measured experimentally and T_D is the temperature at which microbial death occurs. If it is assumed that at T_e the first exponential term in equation (47) is dominant and that a 10°C rise above T_e increases the rate by a factor Q_{10}, A and E may be found from the relationships:

$$E = \frac{T_e(T_e + 10) \ln Q_{10}}{10} \tag{48}$$

$$A = \exp(E/T_e) \tag{49}$$

Assuming that the second exponential term, $A' \exp(-E'/T^2)$, increases by a factor QD_{10} over a range $T_D - 10$°C to T_D and noting that at T_D this term must equal the first, A' and E' are calculated using:

$$E' = \frac{(T_D - 10)^2 T_D^2 \ln QD_{10}}{T_D^2 - (T_D - 10)^2} \tag{50}$$

$$A' = A \exp(-E/T_D) \exp(E'/T_D^2) \tag{51}$$

Method of solution

After Lapidus (1962) a Crank–Nicholson finite difference scheme is employed to solve the system of partial differential equations presented in previous sections. A variable radial grid in which the mesh is finest in the regions of greatest concentration or temperature change (Blair & Peaceman, 1962) and axial steps of 0.05 log units are employed. In nondimensional form, the time increments ranged from 2×10^{-5} in the coupled heat-mass transfer case to 5×10^{-5} in the turbulent isothermal mass transfer system. Step sizes are chosen such that a decrease in step size does not significantly affect the results of the computations. Heat and mass balances over the system show that the results obey the conservation equations.

To obtain a linear system of equations, it is necessary to linearize the saturation kinetic expression. If the axial step size is chosen such that the concentrations at two adjacent points at the same radial position are close, then a linear rate expression for an axial position, $j + 1$, may be obtained from the concentration at a previous axial position, j. For a particular radial and axial position, the linear rate expression has the form:

$$R\{C^j\} = \frac{k_1^* C^j}{1 + k_2^* C^j} = k' C^j + k'' \tag{52}$$

The rate constants, k' and k'', are obtained by linearizing about C^j using an increment, ΔC:

$$k' = \frac{R\{C^j + \Delta C\} - R\{C^j - \Delta C\}}{2\Delta C} \tag{53}$$

$$k'' = R\{C^j + \Delta C\} - k'(C^j + \Delta C) \tag{54}$$

In all computations a ΔC of 0.0001 is employed.

Parameters

A dilute solution of glucose in water at an initial temperature of 20°C is used as the fluid in this study. At this temperature, the binary diffusion coefficient for glucose has been found to be 6×10^{-6} cm^2 s^{-1} (Baillod & Boyle, 1970). From Matson (1974) the glucose diffusivity in the biomass (20°C) is taken to be 1.5×10^{-6} cm^2 s^{-1}.

In order to model typical power plant heat exchanger equipment, a turbulent flow average velocity, v, of 152 cm s^{-1} and r_1 and r_0 of 1.09 cm and 1.27 cm, respectively, are chosen. At this flow rate and tube diameter, the core turbulent diffusivity, E_D, is approximately 0.5 cm^2 s^{-1}.

The friction factor, f, is calculated from the Blausius correlation for $Re < 10^5$ (Bird *et al.*, 1962).

$$f = \frac{0.0791}{Re^{1/4}}$$

For glucose as a substrate, the kinetic parameters in the Monod expression have been evaluated by Kornegay (1969). At 20°C, $k_1 = 0.06$ s^{-1} and $k_2 = 0.0083$ l mg^{-1}. Kornegay's data were chosen because the fluid phase was well-mixed, and, thus, the parameters are minimally altered by mass transfer resistances in the fluid. An intermediate glucose feed concentration of 100 mg l^{-1} was taken as the inlet concentration, c_0.

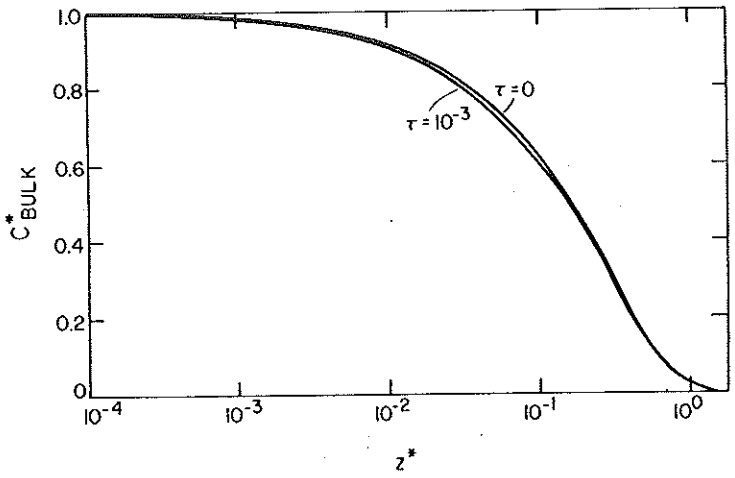

Fig. 2. Dimensionless bulk average concentration vs dimensionless axial distance, laminar flow.

Colton's work with cellulose membranes indicates a membrane partition coefficient near unity for organic solutes (Colton *et al.*, 1971). Therefore, $\alpha = 1$ was employed in this study.

For heat transfer, the viscosity of water as a function of temperature was found using Bingham's equation (Perry, 1963). All other physical and transport properties of water and steam are found from the tables of Keenan *et al.* (1969). The thermal conductivity of the tube wall is chosen to be that of a typical heat exchanger tubing, 304 stainless steel, for which $k_t = 0.163\,\mathrm{J\,cm^{-1}\,s^{-1}\,K^{-1}}$ (Perry, 1963). Since biofilms are typically ~90% water, the thermal conductivity of the slime was taken as that of water.

It is assumed that a thin layer of microorganisms is initially attached, and this initial thickness is 25 μm. Computation is ended when the biofilm attains a maximum depth of 250 μm, on the order of the maximum thicknesses obtained by Kornegay (1969).

In the coupled heat-mass transfer system, Q_{10} and QD_{10} are chosen as 2 and 5, respectively, and T_D taken to be 60°C.

DISCUSSION

For isothermal laminar flow, the dimensionless bulk concentration vs axial distance is plotted in Fig. 2. Note that the axial concentration profile remains virtually unchanged with time and increased slime thickness (the maximum film depth at $\tau = 10^{-3}$ is nearly a factor of 8 greater than the initial slime thickness). This is a result of low diffusivity in the fluid as can be seen from the radial concentration profiles in Fig. 3. In the fluid, there are large concentration gradients with the concentration at the biofilm–fluid interface much lower than that at the centerline. This is characteristic of systems in which fluid phase mass transfer resistance dominates. Thus, the film thickness has little effect on the bulk average concentration profile, since the primary mass transfer resistance is diffusional in the fluid.

Dimensionless bulk concentration versus dimensionless distance for isothermal turbulent flow is shown in Fig. 4. In contrast to the laminar system, as thickness of the biofilm increases, there is initially a

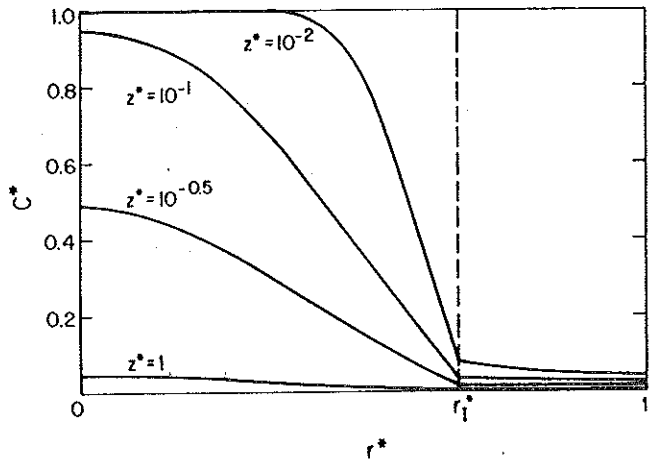

Fig. 3. Dimensionless radial concentration profiles, laminar flow. (Note that the scale in the biofilm is expanded).

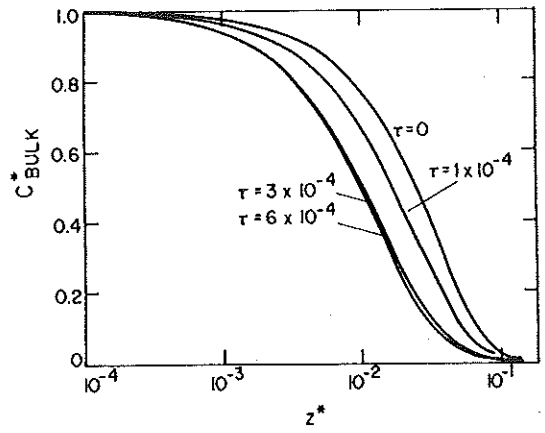

Fig. 4. Dimensionless bulk average concentration vs dimensionless axial distance, turbulent flow.

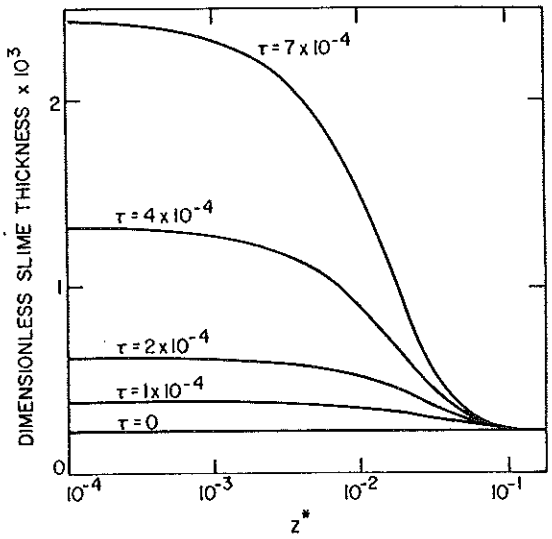

Fig. 6. Dimensionless biofilm thickness vs dimensionless time, turbulent flow.

concommitant change in the bulk concentration profile which indicates that the principal resistance to substrate utilization resides in the biofilm. This conclusion is illustrated by the radial concentration profiles (Fig. 5) which show that the fluid phase is well-mixed, the major change in concentration occuring over the biofilm. Given the parameters employed in this study, it can be seen from Fig. 4 that for lengths up to 30 m ($z^* = 10^{-4}$) the bulk concentration decreases less than 1%. Thus, the biofilm is of nearly constant thickness over this distance.

Laboratory research (Characklis, 1978; Zelver, 1978) indicates that biofilm development in a tube significantly increases frictional resistance which will reduce convective heat transfer resistance. Results indicate, however, that the convective heat transfer resistance accounts for only about 15% of the total heat transfer resistance at steady state.

For simultaneous heat and mass transfer, graphs of space average Nusselt numbers and dimensionless biofilm thicknesses versus dimensionless time are given for axial distances corresponding to 5 and 15 m in Figs 12 and 13, respectively. For temperatures on the outside of the tube greater than that necessary to cause microbial death ($T_D = 60°C$ in this case) biofilm growth will still occur as long as temperatures in the biofilm are below T_D.

Observe that in the 5 m tube (Fig. 12), the biofilm growth rate increases up to $T_0 = 71°C$, and there is a resulting more rapid decrease in average heat flux to the fluid with time. As the fluid and biofilm temperatures rise with increased distance down the tube, T_D is exceeded in the $T_0 = 78°C$ system. Thus, in a 15 m tube (Fig. 13) the space average Nusselt number will be higher in this system than when the saturated steam temperature is 60°C or 49°C. This is shown in the graph of dimensionless slime thickness versus dimensionless axial distance (Fig. 6). From Fig. 7, it is apparent that the growth rate of the biofilm increases up to $\tau = 4 \times 10^{-4}$ at which point the biofilm thickness is approximately 145 μm ($r_1 = 1.09$ cm) up to $z^* = 10^{-4}$ (Fig. 6). It is at this point, too, that the

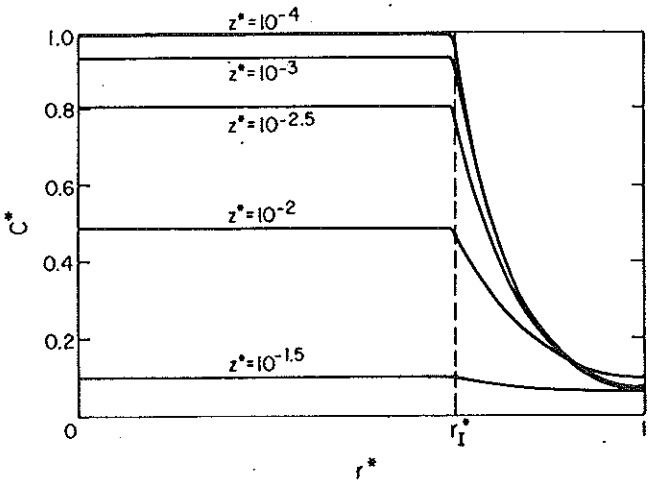

Fig. 5. Dimensionless radial concentration profiles, turbulent flow. (Note biofilm scale is expanded).

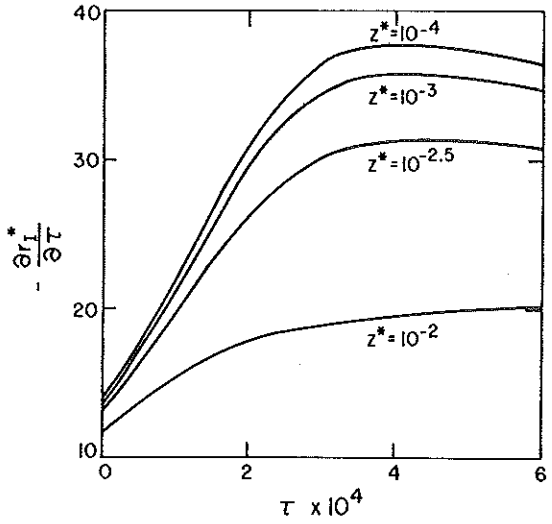

Fig. 7. Dimensionless biofilm growth rate vs dimensionless time, turbulent flow.

bulk concentration profile stops changing with increasing thickness (Fig. 4). Therefore, these results indicate that substrate utilization is initially reaction limited, and as the biofilm grows becomes diffusion limited, the substrate being metabolized over a layer of the biofilm nearest the biofilm–fluid interface. For the parameters used in this study, the active film layer has a thickness of slightly less than 150 μm.

The presence of a biofilm dramatically decreases heat transfer. This is shown in the graphs of dimensionless bulk temperature and space average Nusselt number (Figs 8 and 9, respectively). These figures are calculated for constant biofilm thickness (no mass transfer). As an example of the decrease, given the system described in this paper, a tube with a 250 μm thick biofilm must be more than twice as long as a similar clean tube to affect the same temperature change and total heat transfer to the fluid. In comparing the radial temperature profiles plotted in Figs 10 and 11 for slime thicknesses of 25 and 250 μm, respectively, the temperature difference across the biofilm is a much greater fraction of the total radial temperature rise for the thicker layer than it is in the 25 μm thick biofilm case.

The graph of biofilm thickness vs axial distance for coupled heat–mass transfer is very different from that of isothermal mass transfer as is shown in Fig. 14. While the isothermal thickness is for most practical purposes constant over the region of interest (in which $c \approx c_0$), in the combined heat–mass transfer problem the biofilm thickness initially increases down the tube with temperature rise in the fluid and biofilm. However, when the temperature in the biofilm exceeds that at which the reaction rate begins decreasing, the slime thickness decreases with increasing axial distance. When T_D is attained throughout the biofilm, growth stops completely.

CONCLUSIONS

The results of this study indicate the primary resistances to the transport of heat and mass in a developing tubular biofilm. For laminar flow, utilization of substrate is diffusion limited in the fluid since radial mass transport is solely by molecular diffusion. However, in the turbulent flow system, radial velocity fluctuations yield a much higher effective diffusivity. This results in a well-mixed fluid phase with the principal resistance residing in the biofilm. Initially, film substrate utilization is limited by reaction kinetics. As the biofilm thickens, the bulk concentration profile changes, since an increased microbial mass per length of the tube will metabolize more substrate. Eventually, if growth continues without removal of biofilm, the uptake of substrate becomes diffusion limited, and substrate metabolism takes place over only a portion of the biofilm nearest the slime–fluid interface. As long as the depth of the biofilm at this time is small compared to the tube radius, the bulk concentration

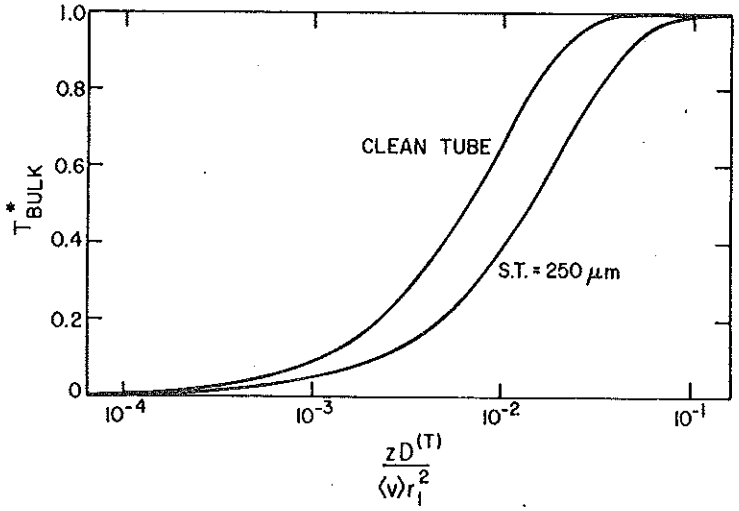

Fig. 8. Dimensionless bulk temperature vs dimensionless axial distance (scaled with respect to molecular thermal diffusivity of water), turbulent flow, $T_i = 20°C$, $T_0 = 100°C$.

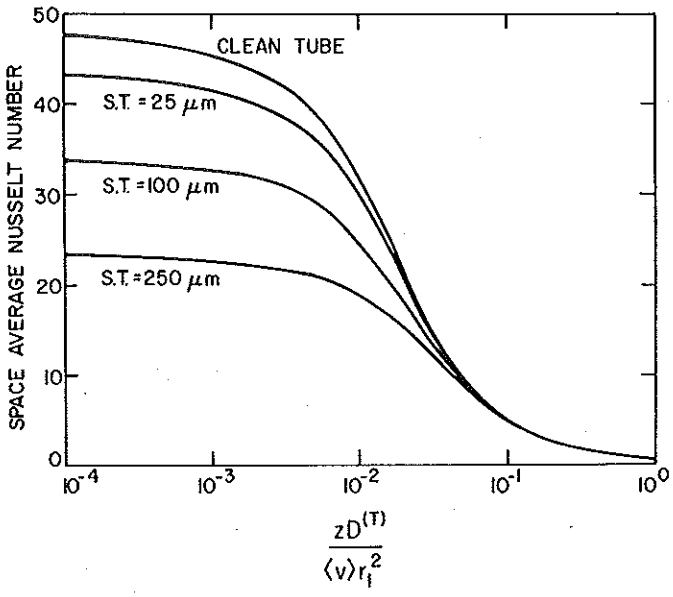

Fig. 9. Space average Nusselt number vs dimensionless axial distance, turbulent flow, $T_i = 20°C$, $T_0 = 100°C$.

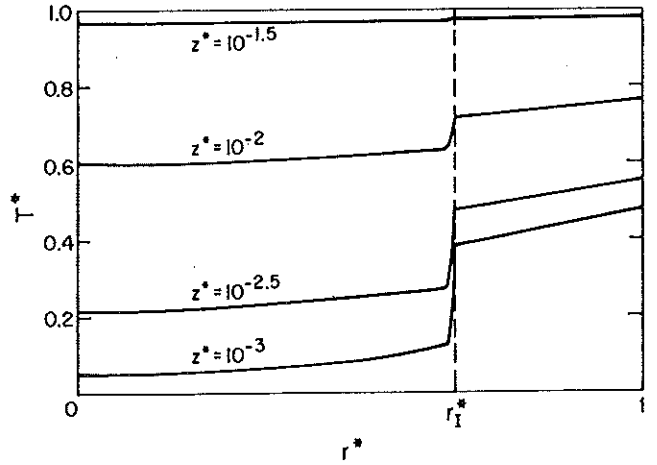

Fig. 10. Dimensionless radial temperature profiles, biofilm thickness = 25 μm $T_i = 20°C$, $T_0 = 100°C$. (Note expanded biofilm scale).

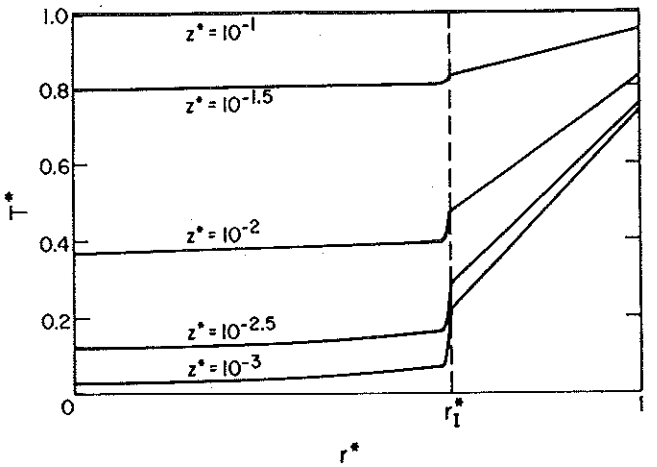

Fig. 11. Dimensionless radical temperature profiles, biofilm thickness = 250 μm $T_i = 20°C$, $T_0 = 100°C$. (Note expanded biofilm scale).

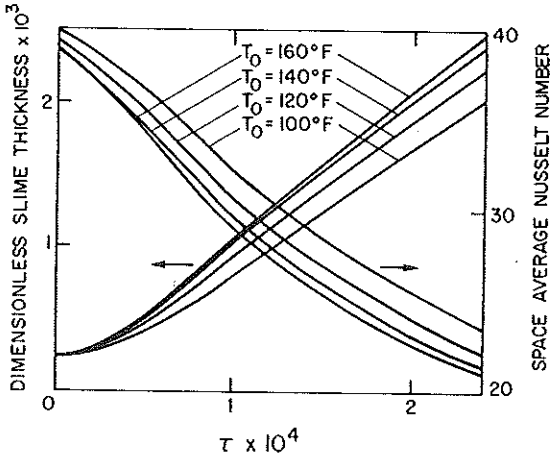

Fig. 12. Dimensionless biofilm thickness and space average Nusselt number vs dimensionless time, $T_i = 20°C$, $Z^* = 1.62 \times 10^{-5}$ ($= 5$ m for $\langle v \rangle = 152$ cm s^{-1}, $r_1 = 1.09$ cm, $D_m = 6 \times 10^{-6}$ cm^2 s^{-1}).

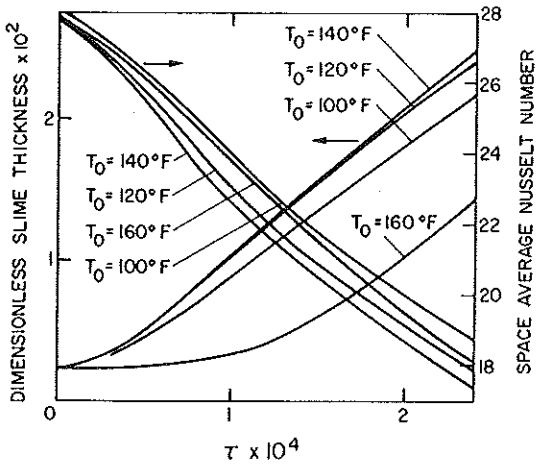

Fig. 13. Dimensionless biofilm thickness and space average Nusselt number vs dimensionless time, $T_i = 20°C$ $Z^* = 5.06 \times 10^{-5}$ ($= 15$ m for $\langle v \rangle = 152$ cm s^{-1}, $r_1 = 1.09$ cm, $D_m = 6 \times 10^{-6}$ cm^2 s^{-1}).

profile will not change significantly with increased biofilm thickness, because the metabolically active layer thickness remains constant.

The presence of a biofilm may seriously decrease heat transfer. For the system presented in this paper, the overall heat transfer coefficient for a tube with a 250 μm thick slime coating may be less than half that of a similar clean tube.

For isothermal mass transfer in most systems of practical interest, the biofilm thickness will only decrease slightly with increase in distance down the tube. In contrast, with combined heat and mass transfer, the biofilm thickness initially increases with increasing axial distance. At some axial distance, the biofilm thickness reaches a maximum because the temperature exceeds that which causes a decrease in reaction rate. At any axial position, the rate of biofilm growth will have a maximum value for a particular saturated steam temperature on the outside of the tube. Likewise, the space average Nusselt number will have a minimum value for some T_i, (not necessarily the same temperature as that for maximum biofilm growth rate). Thus, for a fixed length of heat exchanger tubing with an attached active microbial film, the overall heat transfer coefficient will go through a minimum as T_0 is increased.

These results presented in this paper are of wide applicability in microbial fouling systems. For laminar flow, the bulk concentration is a function of the dimensionless axial distance, the kinetic parameters (k_1^* and k_2^*), and dimensionless time. However, in most cases substrate uptake is diffusion limited in the fluid phase, and the bulk concentration profile remains nearly the same with time. Thus, bulk concentration depends primarily on the dimensionless axial distance and the results given in dimensionless

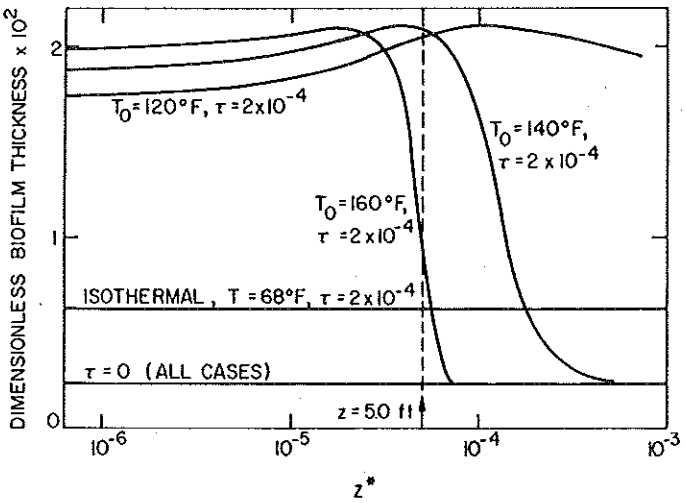

Fig. 14. Dimensionless biofilm thickness vs dimensionless axial distance, $T_i = 20°C$.

form are directly applicable to any laminar system in which the fluid phase diffusivity is the principal resistance.

For turbulent flow, the velocity profile and convective diffusivity are dependent on the Reynolds number and friction factor, and these parameters directly affect the fluid phase heat and mass transport. If the fluid phase is well-mixed and the substrate uptake is biofilm limited, a change in the value of Re and f will not appreciably alter the bulk concentration profile or rate of biofilm growth. It is still necessary to carry out the computation using the particular kinetic parameters for a given system. Consequently, the results for turbulent flow are quantitatively correct only for $k_1^* = 4.75 \times 10^4$ and $k_2^* = 0.83$. Qualitatively, the trends are expected to be the same for any tubular biofouling system.

The transport of heat in tubulent flow depends on the overall heat transfer coefficient. This coefficient in turn depends on the combined resistances of the fluid, biofilm, tube wall, and shell side heat transfer coefficient. Nevertheless, if the biofilm is the primary resistance to the transfer of heat, then curves of space average Nusselt number and bulk temperature should be similar for tubes with the same dimensionless biofilm thickness.

The results given for the coupled heat and mass transfer system are the most difficult to generalize. Calculation of concentration and temperature profiles requires knowledge of the reaction kinetics, heat transfer coefficients, transport properties, and hydrodynamic parameters. Hence, the large number of permutations of the parameters possible would require a substantial amount of computation for complete and systematic quantitative results to be obtained. This dictates that if quantitative estimates of combined heat and mass transfer in microbial fouling systems are required, computations for the specific parameters of interest must be done.

Acknowledgement—Portions of this research were supported by the National Science Foundation (ENG 74-11957).

REFERENCES

Baillod C. R. & Boyle W. C. (1970) Mass Transfer limitations in substrate removal. *J. sanit. Engng Div. ASCE* **96**, 525–545.

Bird W. B., Stewart W. E. & Lightfoot E. N. (1960) *Transport Phenomena*, Wiley, New York.

Blair P. M. & Peaceman D. W. (1962) An experimental verification of a two-dimensional technique for computing performance of gas driven reservoirs. *Numerical Simulation, S.P.E. Reprint Ser.* **11**, 7–15.

Brown G. M. (1960) Heat or mass transfer in a fluid in laminar flow in a circular or flat conduit. *A.I.Ch.E.Jl* **6**, 179–183.

Bruley D. F. & Knisely M. H. (1970) Hybrid simulation oxygen transport in the microcirculation. *Mass Transfer in Biological Systems, A.I.Ch.E., Chem. Engng Prog. Symp. Ser.* No. 99 **66**, 22–32.

Characklis W. G. (1973) Attached microbial growths—I. Attachment and growth. *Water Res.* **7**, 1113–1127.

Characklis W. G. (1973) Attached microbial growths—II. Frictional resistance due to microbial slimes. *Water Res.* **7**, 1249–1259.

Characklis W. G. (1978) Biofilm development and destruction. Final Report, EPRI RP 902-1, Electric Power Research Institute, Palo Alto, California.

Colton C. K. & Drake R. F. (1971) Effect of boundary conditions on oxygen transport to blood flowing in a tube. *Advances in Bioengineering, A.I.Ch.E., Chem. Engng Prog. Symp. Ser.* No. 114 **67**, 88.

Colton C. K., Smith K. A., Merrill E. W. & Farrell P. C. (1971) Permeability studies with cellulosic membranes. *J. Biomed. mater. Res.* **5** 459–488.

Grimsrud L. & Babb A. L. (1966) Velocity and concentration profiles for laminar flow of a Newtonian fluid in a dialyzer. *Chemical Engineering in Medicine., A.I.Ch.E., Chem. Engng Prog. Symp. Ser.* No. 66 **62**, 20–31.

Graetz L. (1883) Ueber die wärmeleitungsfähigkeit von flüssigkeiten *Annln Phys.* (3), **18**, 79–94.

Keenan J. H., Keyes F. G., Hill P. C. & Moore J. G. (1969) *Steam Tables*, Wiley, New York.

Kornegay B. H. (1969) The characteristics and kinetics of fixed film reactors, Ph.D. thesis, Clemson.

Lapidus L. (1962) *Digital Computation for Chemical Engineers*, p. 178, McGraw-Hill, New York.

Levich V. G. (1962) *Physicochemical Hydrodynamics*, p. 144, Prentice Hall, New York.

Lightfoot E. N. (1974) *Transport Phenomena in Living Systems*, p. 334 Wiley-Interscience, New York.

Matson J. V. (1974) Diffusion through microbial aggregates. Ph.D. Thesis, Rice University.

Norrman G., Characklis W. G. & Bryers J. D. (1977) Control of microbial fouling in circular tubes with chlorine. *Devs ind. Microbiol.* **18**, 581–590.

Notter R. H. & Sleicher C. A. (1971) Eddy diffusivity in the turbulent boundary layer near a wall. *Chem. Engng Sci.* **26**, 161–171.

Perry J. H. (editor) (1963) *Chemical Engineer's Handbook*, 4th ed., McGraw-Hill, New York.

Reneau D. D., Bruley D. F. & Knisely M. H. (1969) A digital simulation of transient oxygen transport in capillary-tissue systems (cerebral gray matter). *A.I.Ch.E.Jl* **15**, 916–925.

Reneau D. D. & Knisely M. H. (1971) A mathematical simulation of oxygen transport in the human brain under conditions of counter-current blood flow. *Advances in Bioengineering, A.I.Ch.E., Chem. Engng Prog. Symp. Ser.* No. 114 **67**, 18–27.

Sherwood T. K., Pigford R. L. & Wilke C. R. (1975) *Mass Transfer*, McGraw-Hill, New York.

Waterland L. R., Michaels A. S. & Robertson C. R. (1974) A theoretical model for enzymatic catalysis using asymetric hollow fiber membranes. *A.I.Ch.E.Jl* **20**, 50–59.

Zelver N. (1979) Biofilm development and associated energy losses in water conduits. M.Sc. Thesis, Rice University.